Photoinduced Magnetism and Random Magnetic Anisotropy in Organic-Based Magnetic Semiconductor $V(TCNE)_x$ Films, for $x \sim 2$

Jung-Woo Yoo,[1] R. Shima Edelstein,[1] D. M. Lincoln,[2] N. P. Raju,[1] and A. J. Epstein[1,2]
[1]*Department of Physics, The Ohio State University, Columbus, Ohio 43210-1117, USA*
[2]*Department of Chemistry, The Ohio State University, Columbus, Ohio 43210-1173, USA*
(Received 14 April 2007; published 12 October 2007)

The $V(TCNE)_x$, $x \sim 2$ is an organic-based amorphous ferrimagnet, whose magnetic behavior is significantly affected in the low field regime by the random magnetic anisotropy. It was determined that this material has thermally reversible persistent change in both magnetization and conductivity driven by the optical excitation. Here, we report results of a ferrimagnetic resonance study of the photoinduced magnetism in $V(TCNE)_x$ film. Upon optical excitation ($\lambda \sim 457.9$ nm), the ferrimagnetic resonance spectra display substantial changes in their linewidths and line shifts, which reflect a substantial increase in the random magnetic anistropy. The results reflect the role of magnetic anisotropy in disordered magnets and suggest a novel mechanism of photoinduced magnetism in $V(TCNE)_x$ induced by the increased structural disorder in the system.

DOI: 10.1103/PhysRevLett.99.157205 PACS numbers: 75.90.+w, 75.50.Lk, 75.50.Xx, 76.50.+g

Recently, molecule-based magnets have received growing attention for their new science and also possible application to various spin related devices [1]. A variety of molecule-based magnetic systems display magnetic bistability due to their inherent structural nature and/or their flexibility, and often their bistability can be controlled by optical stimulus [2–4]. A particularly interesting phenomenon is the coexistence of photoinduced magnetism (PIM) and long-range magnetic order, which so far is mainly investigated in two classes of systems: cyanometalate compounds [2,5,6] and the family of $M(TCNE)_x$ (M = Mn, V; $x \sim 2$; TCNE = tetracyanoethylene) magnets [4,7]. Extensive research revealed that PIM in cyanometalate compounds originates from charge transfer induced changes in spin values within the cluster glass model [5,8]. On the other hand, the lack of change in saturation magnetization in $M(TCNE)_x$ by the illumination [4,7,9] suggests a completely different mechanism for PIM. Recent theoretical study suggested that the origin of PIM in $Mn(TCNE)_2$ is a result of change of relative strengths of the double-exchange and superexchange couplings by the charge transfer between metal and ligand due to optical excitation [10]. However, the charge transfer and the change of exchange couplings in this model imply change in saturation magnetization [10].

In this study, we employed photoinduced ferrimagnetic resonance (PIFMR) to investigate the mechanism of PIM in $V(TCNE)_x$ films prepared by chemical vapor deposition (CVD). $V(TCNE)_x$ is a ferrimagnet of antiparallel $(TCNE)^-$ ($S = 1/2$) and V^{2+} ($S = 3/2$) spins with magnetic ordering temperature $T_c \sim 400$ K [11]. Detailed transport studies indicate that the material is a semiconductor with an energy gap ~0.5 eV between spin polarized valence and conduction bands [12–15]. It was reported that $V(TCNE)_x$ exhibits concomitant photoinduced magnetic and electrical phenomena upon optical stimulus [7]. Both the magnetization and conductivity show persistent and thermally reversible change induced by the $\pi \rightarrow \pi^*$ excitation in $(TCNE)^-$ anions [7]. Under illumination, there is a substantial decrease in magnetization of $V(TCNE)_x$ at low field, though the saturation magnetization remains the same as that of the ground state [7]. The light-induced magnetism and conductivity have long lifetime at low T, and the effects are erased when the illuminated sample is warmed up to 250 K [7]. The optical investigation suggested light-induced activation to a metastable state associated with small structural changes [4,7]. This PIFMR study shows that random magnetic anisotropy (RMA) plays a central role in photoinduced magnetic phenomena in $V(TCNE)_x$. Upon optical excitation ($\lambda \sim 457.9$ nm), the ferrimagnetic resonance spectra display a substantial increase in linewidth and a shift in the resonance field depending on the orientation of the applied magnetic field. This result shows that the PIM in $V(TCNE)_x$ originates from the enhanced RMA induced by increased structural disorder caused by the light excitation.

Metal-$(TCNE)_x$ are one class of hybrid magnets that are composed of spin carrying organic radicals and transition metal ions [16–18]. The magnetic order of these materials is based on direct exchange between the unpaired electrons in π^* orbitals of organic radicals [19] and the spins in the transition metal ions. Generally, these materials have a disordered structure leading to RMA. This random spatial distribution of the local anisotropy axis should significantly affect the magnetic properties of these systems. In particular, several chemical routes have been established to form $V(TCNE)_x$, introducing various residual solvents in the system, which introduce significant effects on magnetic coupling and magnetic anisotropy [20–23]. Recently, solvent-free thin films of $V(TCNE)_x$ synthesized via the CVD method have shown to have greatly diminished oxygen/moisture sensitivity and increased local structural or-

der compared to the solution prepared powder samples [24,25]. Extended x-ray absorption fine structure studies show octahedral coordination of N around V in CVD films with robust V-N length [2.084(5) Å] [25]. However, the absence of crystalline x-ray diffraction peaks indicates a disordered structure leading to RMA [24,25].

The CVD deposited solvent-free films of $V(TCNE)_x$ were prepared in an Ar filled glove box ($O_2 < 0.1$ ppm, $H_2O < 1.0$ ppm) [24]. The ~500 nm thick samples were deposited on thin glass substrates ($5 \times 2 \times 0.1$ mm^3). The ferrimagnetic resonance (FMR) measurements were performed on a Bruker ESP300 (X-band, 9.6 GHz) ESR spectrometer using a TE_{102} resonant cavity. The dc magnetization was recorded on a Quantum Design MPMS-5 SQUID magnetometer. An Ar-ion laser (Coherent I300) with a fiber optic coupling was used for illumination. Samples for the measurements were sealed in ESR quartz tubes under vacuum for protection from oxidation. Diamagnetic corrections were made for dc magnetic measurements.

The time dependent evolution of FMR spectra under illumination is illustrated in Fig. 1. The angle between the normal to the film and the external field was set to $\theta \sim 54.7°$, where the spectrum collapses to a single resonance as the effects of demagnetization and uniaxial anisotropy of films are essentially eliminated [see Eq. (1) below]. Upon illumination [$\lambda \sim 457.9$ nm, light intensity (I) ~20 mW/cm^2, $T = 30$ K], the FMR absorption spectrum became substantially broader and the resonance field was shifted to a lower value. The intensities of the first integration of the FMR spectra fit well to Lorentzian curves. The time dependence of the linewidth (FWHM) and resonance field (obtained from spectra in Fig. 1) during illumination are displayed in the inset of Fig. 1. At 30 K, the linewidth is increased by twofold and the resonance field is decreased by 10 Oe upon illumination for 1 h ($\lambda \sim 457.9$ nm, $I \sim$ 20 mW/cm^2). The light-induced FMR spectra were recovered to the initial FMR lines, when the sample was warmed to 250 K and cooled back to initial T. In contrast, the dc magnetization of the film at external field 3500 Oe is almost saturated and does not show any change due to the illumination. However, the FMR absorption spectra show substantial change in spin dynamics in the system caused by the illumination. Furthermore, increased linewidth in FMR spectra suggests a slowing down of spin relaxations and a decrease in effectiveness of exchange narrowing. This could be attributed to either increased fluctuation of exchange coupling and/or increased RMA.

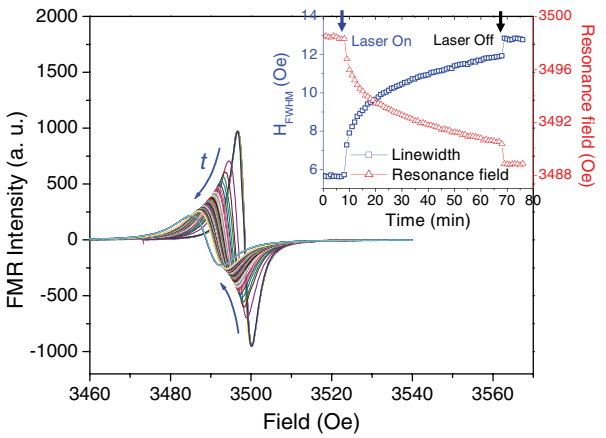

FIG. 1 (color online). Evolution of FMR spectrum under light illumination ($\lambda \sim 457.9$ nm, $I \sim 20$ mW/cm^2, at 30 K). Inset: the linewidth and resonance field obtained by the Lorentzian fit of the FMR spectra.

Figure 2 displays typical FMR spectra of CVD deposited $V(TCNE)_x$ film for various orientations of the external magnetic field with respect to the normal to the plane of film for both ground and photoexcited states at 30 K. For a measurement of the photoexcited state, the sample was illuminated for 2 h with $\lambda \sim 457.9$ nm and $I \sim$ 20 mW/cm^2. When $4\pi M \ll H$ (M is the magnetization and H is the applied magnetic field), the magnetization of films lie nearly along the applied field for all orientations. For a small anisotropy field H_A and $4\pi M - H_A \ll H_r$, the angular dependence of the resonance behavior for a planar sample can be expressed by a simple equation [26–28].

$$H \simeq H_r + \left(2\pi M - \frac{H_A}{2}\right)(2 - 3\sin^2\theta), \qquad (1)$$

where θ is the angle from the normal to the plane of the film to the external magnetic field, and H_r is the internal

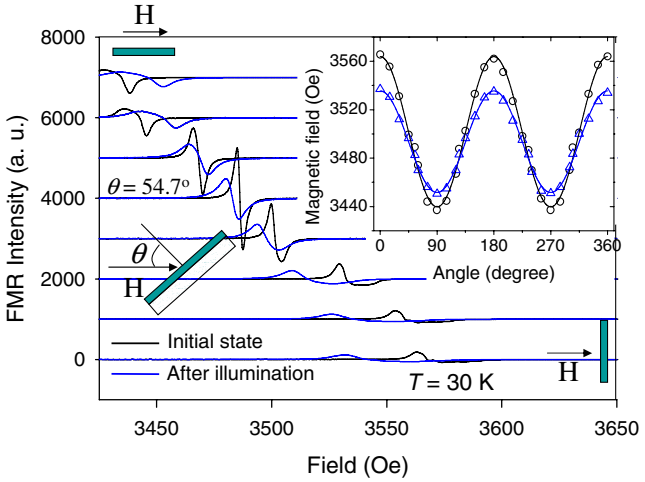

FIG. 2 (color online). Effects of illumination on angular dependence of FMR spectra of $V(TCNE)_x$ film at 30 K for the angle ($\theta = 90°, 75°, 60°, 55°, 45°, 30°, 15°, 0°$ from top to bottom) from the normal to the plane of the film to the external magnetic field (black line: ground state; blue line: after illumination with $\lambda \sim 457.9$ nm, $I \sim 20$ mW/cm^2 for 2 h). Inset: angular dependence of line shift for a particular FMR line of $V(TCNE)_x$ film for both ground (○) and photoexcited (△) states. Solid lines are fits to Eq. (1).

resonance field (i.e., the field at which resonance will occur in the absence of any shape effects). The internal resonance field can be described by an effective g value, $g_{\text{eff}} = \hbar\omega/\mu_B H_r$, where $\hbar$ is Planck's constant, ω is the spectrometer operating frequency, and μ_B is the Bohr magneton. H_A is a perpendicular uniaxial anisotropy field. As the $V(TCNE)_x$ has an amorphous structure, crystalline anisotropy is negligible and RMA mainly accounts for H_A, which can be assumed to be independent of the angle.

One can see that several spectral features in Fig. 2 can be observed when θ differs from 54.7°. These features correspond to nonuniform regions with distinct $4\pi M - H_A$ values within the sample, and collapse to a single spectrum at $\theta = 54.7°$. Similar angular dependent FMR spectra in $V(TCNE)_x$ films were reported previously with a larger number of resonances due to inhomogeneity of samples [28]. The inset of Fig. 2 shows the angular dependence of the resonance field for a specific FMR line (the most pronounced resonance spectrum) and fit to Eq. (1). Note that there is a substantial reduction of angle dependent line shift after the light irradiation. Such a light-induced shift of the resonance field suggests a substantial increase of H_A, because the magnetization at $H \sim 3500$ Oe is almost identical for both ground and photoexcited states according to the SQUID measurements [7,9].

The T dependence of H_A can be obtained from the T dependence of the resonance fields for particular orientations, $\theta = 0°$, 90°, and 54.7°, which reduce to $H(0°, T) = H_\perp \simeq H_r + 4\pi M - H_A$, $H(90°, T) = H_\parallel \simeq H_r - 2\pi M + \frac{H_A}{2}$, and $H(54.7°, T) \simeq H_r \simeq 1/3(H_\perp + 2H_\parallel)$, respectively. $M(T)$ was estimated from the total integrated intensity of FMR spectra with values scaled using dc magnetic measurement results ($M = 17.7$ G at 5 K and 3500 Oe). Figure 3 shows temperature dependence of the resonance field of the most pronounced FMR line for angles $\theta = 0°$, 54.7°, and 90° [Fig. 3(a)], subtracted $4\pi M(T) - H_A(T) \simeq H(0°, T) - H(54.7°, T)$ [Fig. 3(b)], and resultant $H_A(T)$ [Fig. 3(c)] for both ground and photoexcited states. The measurements for photoexcited states were made after illumination with $\lambda \sim 457.9$ nm, $I \sim 20$ mW/cm^2 for 2 h at 30 K. Fitting the Bloch law [$M_s(T) = M_s(0)(1 - BT^{2/3})$] to the total integrated intensity of FMR spectra is employed to subtract $M(T)$. In a phenomenological approach, $H_A = 2K/M$, where K is an anisotropy constant of RMA. The anisotropy constant increases linearly as T is lowered [Fig. 3(c)]. This behavior is similar to that experimentally observed in a spin glass system with a relation $K(T) = K(0)[1 - (2/3)T/T_f]$, where T_f is the spin freezing temperature [29] and is qualitatively similar to the theoretical prediction for spin glasses [30]. Note that a substantial increase of the anisotropy field H_A caused by the illumination at 30 K can be observed over the wide range of temperature. At 10 K, the anisotropy field ($H_A \sim$ 143 G) extracted from the most pronounced resonance line increased by 17% after the illumination.

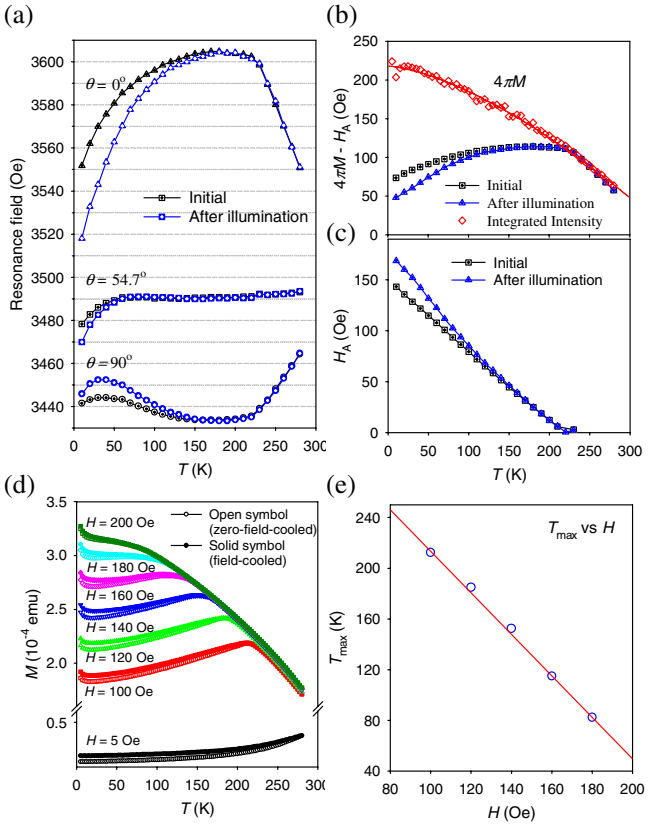

FIG. 3 (color online). (a) Light-induced effect on the temperature dependence of resonance field for the most pronounced FMR line at $\theta = 0°$, 54.7°, and 90° (Black line and symbol: ground state; Blue line and symbol: photoexcited state, measured after illumination with $\lambda \sim 457.9$ nm, $I \sim 20$ mW/cm^2 for 2 h at 30 K). (b) Extracted $4\pi M - H_A$ from selected FMR line between $\theta = 0°$ and 90° for both ground and photoexcited states. Red symbol shows total integrated intensity of FMR spectra and red line is Bloch function fit to the total integrated intensity of FMR spectra. (c) Temperature dependence of H_A after substraction with Bloch function fit to the total integrated intensities of FMR absorptions for both ground and photoexcited states. (d) Field-cooled and zero-field-cooled dc magnetization for an applied magnetic field 100, 120, 140, 160, 180, and 200 Oe. (e) Magnetic field dependence of the zero-field-cooled peak temperatures (T_{max}).

In amorphous magnets, when the anisotropy energy is small compared to the exchange energy, Chudnovsky *et al.* predicted a formation of different magnetic phases in the material according to the strength of an applied magnetic field [31]. Depending on the degree of anisotropy, a correlated spin glass (CSG) phase may appear at low field, while at the intermediate field small domains with a local correlated anisotropy axis, the ''so-called'' ferromagnetic wandering axis (FWA) phase, may be formed. At high enough field, the system will be nearly a collinear ferromagnetic phase. The main difference between a spin glass and a CSG is the origin of spin freezing. In a spin glass, the freezing of spin is a consequence of random magnetic interaction.

Mean field theory produces the AT (Almeida-Thouless) instability line, $\delta T_f \propto H^{2/3}$ for Ising spin glasses [32], and transverse freezing with the GT (Gabay-Toulouse) line, $\delta T_f \propto H^2$, followed by the AT longitudinal freezing line for Heisenberg spin glasses [33]. On the other hand, the spin freezing of CSG relies on random magnetic anisotropy. Figure 3(d) shows the temperature dependence of field-cooled and zero-field-cooled dc magnetization. At low field, $H = 5$ Oe, M slowly increases as T increases and does not show peaks until 280 K. The ac susceptibility has similar T dependent behavior with no frequency dependence below 300 K [34]. At relatively high fields ($H >$ 100 Oe), M decreases monotonically as T increases, suggesting substantial excitation of spin waves with low wave vectors, which is expected for the FWA phase of disordered $V(TCNE)_x$ [21,34]. As T is decreased, M peaks at a temperature, T_{max} and is suppressed as T is lowered further. The M exhibits weak irreversibility, given by the deviation between field-cooled and zero-field-cooled magnetization below a particular $T_{irr} \sim T_{max}$. As the intensity of the applied magnetic field increases, the T_{max}, where the spins start to freeze, shifts to lower temperatures following a linear relation $T_{max} = a - bH$ [Fig. 3(e)], which was earlier reported for another amorphous magnetic system [35]. This variation of the position of peaks may then be a direct consequence of RMA, which increases linearly as T is lowered, and makes CSG distinct from the spin glass, where the position of peaks in zero-field-cooled curves follows the AT line and/or the GT line.

In conclusion, the persistent PIM in $V(TCNE)_x$ films was probed via PIFMR studies. The responses of line shift and linewidth of FMR spectra of $V(TCNE)_x$ films to the illumination are well correlated to the light-induced increase of RMA resulting from increased structural disorder. Our results and conclusions contradict the theoretical study for the mechanism of the PIM in related $Mn(TCNE)_2$ magnets [10]. The results also display the role of magnetic anisotropy in amorphous magnets providing distinction between spin glass and CSG. The PIFMR study of $V(TCNE)_x$ film demonstrates a new mechanism for PIM in organic and/or molecule-based magnets, beyond changing spin numbers and exchange couplings, and suggests a different approach for the optical control of magnetic properties in materials.

This work was supported in part by the AFOSR Grants No. F49620-03-1-0175 and No. FA9550-06-1-0175, DOE Grants No. DE-FG02-01ER45931 and No. DE-FG02-86ER45271.

[1] A. J. Epstein, MRS Bull. **28**, 492 (2003).
[2] O. Sato, T. Iyoda, A. Fujishima, and K. Hashimoto, Science **272**, 704 (1996).
[3] P. Gütlich and H. Goodwin, Top. Curr. Chem. **233**, 1 (2004).
[4] D. A. Pejaković, C. Kitamura, J. S. Miller, and A. J. Epstein, Phys. Rev. Lett. **88**, 057202 (2002).
[5] D. A. Pejaković, J. L. Manson, J. S. Miller, and A. J. Epstein, Phys. Rev. Lett. **85**, 1994 (2000).
[6] S. Ohkoshi *et al.*, J. Am. Chem. Soc. **128**, 5320 (2006).
[7] J. W. Yoo *et al.*, Phys. Rev. Lett. **97**, 247205 (2006).
[8] T. Kawamoto, Y. Asai, and S. Abe, Phys. Rev. Lett. **86**, 348 (2001).
[9] See EPAPS Document No. E-PRLTAO-99-018742 for $M(H)$ at 5 K for both ground and photoexcited states. For more information on EPAPS, see http://www.aip.org/pubservs/epaps.html.
[10] S. Erdin and M. van Veenendaal, Phys. Rev. Lett. **97**, 247202 (2006).
[11] J. M. Manriquez *et al.*, Science **252**, 1415 (1991).
[12] V. N. Prigodin *et al.*, Adv. Mater. **14**, 1230 (2002).
[13] N. P. Raju *et al.*, J. Appl. Phys. **93**, 6799 (2003).
[14] C. Tengstedt *et al.*, Phys. Rev. B **69**, 165208 (2004).
[15] C. Tengstedt *et al.*, Phys. Rev. Lett. **96**, 057209 (2006).
[16] J. Zhang *et al.*, Angew. Chem., Int. Ed. Engl. **37**, 657 (1998).
[17] E. B. Vickers, T. D. Selby, and J. S. Miller, J. Am. Chem. Soc. **126**, 3716 (2004).
[18] E. B. Vickers, I. D. Giles, and J. S. Miller, Chem. Mater. **17**, 1667 (2005).
[19] A. Zheludev *et al.*, Angew. Chem., Int. Ed. Engl. **33**, 1397 (1994).
[20] W. B. Brinckerhoff, J. Zhang, J. S. Miller, and A. J. Epstein, Mol. Cryst. Liq. Cryst. **272**, 195 (1995).
[21] P. Zhou, B. G. Morin, J. S. Miller, and A. J. Epstein, Phys. Rev. B **48**, 1325 (1993).
[22] P. Zhou, S. M. Long, J. S. Miller, and A. J. Epstein, Phys. Lett. A **181**, 71 (1993).
[23] M. S. Thorum, K. I. Pokhodnya, J. S. Miller, and A. J. Epstein, Polyhedron **25**, 1927 (2006).
[24] K. I. Pokhodnya, A. J. Epstein, and J. S. Miller, Adv. Mater. **12**, 410 (2000).
[25] D. Haskel *et al.*, Phys. Rev. B **70**, 054422 (2004).
[26] M. J. Pechan, M. B. Salamon, and I. K. Schuller, J. Appl. Phys. **57**, 3678 (1985).
[27] M. J. Pechan, M. B. Salamon, and I. K. Schuller, J. Appl. Phys. **59**, 3302 (1986).
[28] R. Plachy *et al.*, Phys. Rev. B **70**, 064411 (2004).
[29] S. Schultz, E. M. Gullikson, D. R. Fredkin, and M. Tovar, Phys. Rev. Lett. **45**, 1508 (1980).
[30] K. W. Becker, Phys. Rev. B **26**, 2394 (1982).
[31] E. M. Chudnovsky, W. M. Saslow, and R. A. Serota, Phys. Rev. B **33**, 251 (1986).
[32] J. R. L. de Almeida and D. J. Thouless, J. Phys. A **11**, 983 (1978).
[33] M. Gabay and G. Toulouse, Phys. Rev. Lett. **47**, 201 (1981).
[34] K. I. Pokhodnya, D. A. Pejaković, A. J. Epstein, and J. S. Miller, Phys. Rev. B **63**, 174408 (2001).
[35] J. Tejada *et al.*, Phys. Rev. B **42**, 898 (1990).